NACA RM E56A24

RESEARCH MEMORANDUM

DESIGN OF TWO TRANSPIRATION-COOLED STRUT-SUPPORTED TURBINE ROTOR BLADES

By Ernst I. Prasse, John N. B. Livingood, and Patrick L. Donoughe

Lewis Flight Propulsion Laboratory
Cleveland, Ohio

NATIONAL ADVISORY COMMITTEE
FOR AERONAUTICS

WASHINGTON

April 25, 1956

NACA RM E56A24

NATIONAL ADVISORY COMMITTEE FOR AERONAUTICS

RESEARCH MEMORANDUM

DESIGN OF TWO TRANSPIRATION-COOLED STRUT-SUPPORTED TURBINE ROTOR BLADES

By Ernst I. Prasse, John N. B. Livingood, and Patrick L. Donoughe

SUMMARY

Design details of two transpiration-cooled strut-supported turbine rotor blades are presented. Both designs are based on present-day gas temperatures. One design utilizes a sintered blade shell, the other a wire blade shell. Details of the strut designs and considerations involved in selection of strut material are presented for both blades. Ideal variations in coolant flow and shell permeability requirements are determined.

Because of fabrication difficulties that might be encountered in attaining the ideal variations, calculations are also presented for several prescribed permeability variations. For the sintered-shell blade a single uniform chordwise and spanwise permeability obtainable at the time of design was considered. The excess amount of cooling air over that required ideally was about 65 percent for this blade. It is more likely that variations in shell permeability may be obtainable with the use of porous wire cloth than with porous sintered material. Therefore, four cases were considered involving constant chordwise and both constant and variable spanwise prescribed permeabilities for the wire-shell blade. The excess amount of cooling air over that required ideally ranged from 50 to 230 percent for the four cases.

Sizes of orifices located in the blade bases for metering the cooling air ranged from 0.047 to 0.110 inch in diameter for both sintered-shell and wire-shell blades.

INTRODUCTION

Many analytical studies indicate the potential of transpiration cooling for cooling components of gas-turbine engines designed for operation at high turbine-inlet temperature. Two general types of porous material (porous sintered metal powder and porous wire cloth) have received consideration for use as shells of transpiration-cooled turbine blades.

Several types of porous sintered turbine blades have been designed and tested under static conditions (refs. 1 to 3). A turbine rotor blade with shell of porous wire cloth was designed, fabricated, and tested at the NACA Lewis laboratory (ref. 4). The shell was wrapped around a support member, or strut, and joined along the trailing edge. Orifices in the blade base were used to meter the cooling air to each internal passage.

During engine tests of the blade reported in reference 4, the wire-cloth shell split along the trailing edge near the blade tip. This failure may have been caused by insufficient flow of cooling air to the trailing-edge region of the blades. It is generally difficult to cool the trailing-edge region adequately in cooled turbine blades. In addition, when the blade of reference 4 was designed, no method was available for determining the spanwise variation in the cooling-air pressure in the rotor blade passages. A knowledge of the cooling-air pressure is necessary to determine the coolant-flow rate through the porous wall at any position on the blade surface. A method for calculating the spanwise variation in cooling-air pressure in the passages of a transpiration-cooled rotor blade was subsequently developed and reported in reference 5. Recently, a procedure was completed (ref. 6) for the design of transpiration-cooled strut-supported turbine rotor blades, which incorporates this analysis.

Development work is still required to obtain transpiration-cooled turbine blades that can operate at the high temperature and stress levels associated with engines designed for high-altitude, supersonic Mach number flight, while using only the small amount of cooling air required in theory. Initial tests of proposed blade designs must usually be made in a current engine. Such tests provide an experimental check of theories used in the blade design as well as an indication of blade durability. As a step toward the goal of providing transpiration-cooled turbine rotor blades for operation at high gas temperature, the NACA has designed two blades for the sea-level static conditions of a current turbojet engine, using the procedure of reference 6. A sketch of one such blade is presented in figure 1(a), and layouts of the strut cross sections for the two blades are shown in figures 1(b) and (c). If fabricated, these blades could be tested in a current engine.

These blade designs were intended (1) to determine the variations in shell permeability and quantities of cooling air that would be required ideally to maintain a prescribed shell temperature, (2) to determine the cooling-air quantities and orifice diameters for specified variations in shell permeability to which the designer may be limited in practice by shell fabrication considerations, (3) to illustrate details of the design procedure of reference 6, and (4) to consider strut and shell material selection and fabrication methods that might be practicable if attempts to fabricate the blades were made. The purpose of the present report is to present this information.

[redacted]

In the blade designs considered herein, one blade utilizes a shell of porous sintered metal powder and the other a shell of porous wire cloth. The strut and shell of a blade cannot be designed independently; for the sake of clarity, however, the discussions of the strut design and shell design for each blade are separated.

SYMBOLS

A	cross-sectional area, sq ft
b	chordwise peripheral width of coolant passage, ft
D_h	coolant-passage hydraulic diameter, ft
f	function
K	permeability coefficient, sq ft or sq in.
L	coolant-passage length, ft
p	static pressure, lb/sq ft
Re	gas Reynolds number, $\rho Wy/\mu$
T	temperature, $^{\circ}F$ or $^{\circ}R$
v	cooling-air velocity through porous wall, ft/sec
W	gas velocity relative to blade, ft/sec
w	weight flow of cooling air, lb/sec
x	spanwise distance from blade base, ft
y	peripheral distance from blade leading edge, ft
μ	absolute viscosity (based on porous-wall temperature), lb/(ft)(sec)
ρ	density, lb/cu ft
σ	centrifugal stress, psi
τ	porous-blade shell thickness, ft or in.
φ	temperature-difference ratio, $(T_g - T_w)/(T_g - T_c)$

[redacted]

Subscripts:

a	cooling-air supply at blade base
c	cooling air
cr	critical
e	external gas flow
g	effective gas
i	internal coolant flow
le	leading edge
r	coolant-passage entrance (blade root)
t	blade tip
to	total cooling-air flow to turbine rotor
w	porous wall

DESIGN OF SINTERED-SHELL BLADE

As noted in the INTRODUCTION, several types of porous sintered turbine blades for static tests have been designed and tested. However, no sintered-shell rotor blades have been designed. Since a rotor blade design differs markedly from that of a stator blade, the NACA undertook the design of such a blade. As discussed in reference 6, lack of strength of porous materials necessitates the use of an internal load-carrying member (strut) to which the porous shell may be attached. Details of such a design will now be discussed.

Strut

Choice of the strut material usually depends mainly on imposed stresses. Initial estimates indicate that, for the design condition, the maximum centrifugal stress on the strut is about 30,000 psi. In addition to this strength requirement, the choice of strut material may be influenced by the blade fabrication method (e.g., the shell and strut may be sintered together in a high-temperature furnace). Strength tests at 1000° F of cast bar stock that had been exposed to sintering conditions are reported in reference 7 (p. 71). Results indicated that S-816 alloy could withstand 60,000-psi stress at this temperature.

These tests were discontinued after 101 and 156 hours with no rupture. With S-816 as the strut material, the stress-ratio factor (see ref. 6 for a discussion of stress-ratio factor) employed in the present design would then be approximately 2. The choice of strut material can thus be greatly influenced by the fabrication method.

The airfoil and base sections of the strut may be cast integrally, the cooling-air passages and instrumentation holes being formed in casting. The base serrations for attaching the blade to the turbine rotor would be ground after assembly of the strut and shell.

In the preliminary design of the strut, the centers of gravity of each chordwise section were stacked on a radial line to reduce bending stresses due to centrifugal force. In the final strut design, the centers of gravity of the chordwise sections of the strut were tilted slightly toward the suction surface to compensate partially for the gas bending load. Layouts of chordwise cross sections of the strut for this design at three spanwise positions (root, mean, and tip) are shown in figure 1(b). To simplify the design and fabrication of the strut, the strut was designed so that the inner contour of the blade shell coincided at each spanwise position with the contour of a standard uncooled blade of a current turbojet engine.

There are 12 strut fins, each approximately 0.060 inch wide, to provide adequate area for the attachment of the sintered shell to the strut. Hence, with the shell in place, five cooling-air passages are formed on each blade surface, in addition to passages at the blade leading and trailing edges (fig. 1(b)). The maximum width of porous shell between fins is about 0.3 inch for passages along the blade suction and pressure surfaces; the overhang of the shell forming the blade leading- and trailing-edge passages is not more than 0.2 inch. The widths between fins are less than the corresponding values for the blade design of reference 4. With these widths, the shell should be stiff enough to minimize vibrations between the fins. More serious shell vibration problems may exist near the blade leading and trailing edges; however, these problems were not considered in the present design.

The geometry of the cooling-air passages, necessary for the calculations of the blade shell design, was obtained by measurements of enlarged layouts of strut cross sections. These layouts were taken at five spanwise positions along the blade. Typical examples of the geometry are given in table I. Three typical cooling-air passages, discussed in the following section, are used for the examples. The measured values of passage flow area, passage width, and hydraulic diameter are tabulated

against spanwise distance from the blade base. To simplify strut fabrication as well as the calculation procedure for the blade shell, the strut is designed so that nearly linear spanwise variations in passage flow area result. The initial strut design may lead to erratic cooling-air pressure and flow variations. Alterations of the strut design (changes in passage cross-sectional-area distribution) may then be required. Such alterations were not necessary in the present design.

Shell

Design conditions. - In transpiration-cooling processes, the principal defining parameters are

$$1 - \varphi = \frac{T_w - T_c}{T_g - T_c} \tag{1}$$

the gas Reynolds number Re, and the wall temperature T_w. The ideal cooling-air flow ρv may be expressed in terms of these parameters as follows:

$$\rho v = f(\varphi, Re, T_w) \tag{2}$$

Specification of the temperatures in equation (1) and the Reynolds number, then, essentially determines the ideal coolant flow by equation (2).

Sintered metal powder (e.g., stainless-steel powder), when attached to the struts, should be able to withstand temperatures T_w of 1000° to 1200° F. Use of such shell temperatures for design conditions (gas temperature T_g = 1425° F and coolant temperature T_c = 180° F) would result in extremely small required coolant flows. It was decided, therefore, to overcool the shell in order to increase the amount of coolant required. The shell temperature T_w was therefore prescribed as 600° F. Substitution in equation (1) of T_g = 2250° F, T_w = 1200° F, and T_c = 750° F (representative values for a high-temperature and high flight Mach number application) yields a value of $1 - \varphi$ similar to that obtained for the design conditions. Because of this, the lower value of T_w should partially simulate the cooling-air flow required at high gas temperature, although the Reynolds number and shell temperature are different in the high-temperature application.

Tests at the lower wall temperature (600° F) would provide data useful in verifying heat-transfer and coolant-flow theories used in the blade design. Strength tests made by reducing or eliminating cooling-air flow to the blade would provide an initial estimate of blade

durability. Such tests would not be an adequate substitute for durability tests at high temperature, however, because the thermal stresses would probably be different for different wall temperatures.

The value of T_w is needed to calculate the ideal variations in shell permeability-to-thickness ratio K/τ. In addition to the value of T_w, the gas pressure and velocity on the outside blade surface are also needed.

Distribution of gas pressure and velocity. - Chordwise distributions of gas pressure and velocity relative to the blade were calculated at three spanwise positions (root, mean, and tip) by the method explained in reference 6. These distributions are presented in figure 2. The points of transition from laminar to turbulent flow around the blade surfaces were taken as those points where the pressure gradients first vanish; in most cases, these points are the points of minimum pressure. With the use of this criterion and figure 2, it is found that cooling passages 1 to 5 lie in the laminar gas-flow region and passages 6 to 12 lie in the turbulent gas-flow region. Values of the Euler numbers $\left(\frac{y}{W}\frac{dW}{dy}\right)$ for the laminar flow passages are calculable from the information in figure 2.

Variation of ideal coolant flow and permeability-to-thickness ratio. - The ideal cooling-air flow ρv required to maintain a uniform shell temperature of 600° F was calculated for the 12 cooling-air passages. For these calculations, as indicated previously, the effective gas temperature was taken as 1425° F; the cooling-air temperature was assumed to vary linearly through each passage by the relation $T_c = 180 + 644x$ °F, representing an increase in cooling-air temperature from blade root to tip of about 200° F (see ref. 6). The ideal ρv values were determined at the three spanwise positions for the passages by use of the appropriate theory in reference 6. The spanwise distributions were obtained for each passage by plotting these values against spanwise distance; typical examples are shown in figure 3(a). In this figure and through the rest of this report passages 1, 4, and 10 are used as typical examples (the leading-edge passage, midchord suction-surface passage, and midchord pressure-surface passage, respectively).

With the cooling-passage geometries known, the spanwise variations in the gas pressure along each passage available from the information in figure 2 (examples shown in fig. 3(b)), and the spanwise variations in the ideal cooling-air flow known, the spanwise variations in the cooling-air pressure for the passages were calculated (examples shown in fig. 3(c)). Finally, the spanwise variations in shell permeability-to-thickness ratio K/τ were calculated, by substituting $T_w = 1060°$ R

[redacted]

(600° F) into the flow correlation for a typical sintered material given by equation (12) of reference 6, and solving for K/τ:

$$\frac{K}{\tau} = 0.0001972 \frac{\rho v}{(p_i^2 - p_e^2)^{2/3}} \quad (3)$$

The spanwise variations in K/τ for all 12 blade passages are shown in figure 4.

Compromises in permeability-to-thickness ratio. - From figure 4, it is evident that large variations in K/τ are required in both the chordwise and spanwise directions if a uniform shell temperature of 600° F is to be maintained. Under current techniques for fabrication of sintered blade shells, such variations in permeability-to-thickness ratio K/τ are extremely difficult, if at all possible, to obtain. Therefore, a constant and attainable value of K was specified; this value is 8×10^{-10} square inch (5.56×10^{-12} sq ft), the minimum value that could be fabricated with adequate control of random variations. With this constant value of K, the only possible way to achieve variations in K/τ similar to those shown in figure 4 would be to vary the shell thickness τ in both the chordwise and spanwise directions. The required chordwise variations in K/τ can be partially achieved, however, by use of the constant chordwise K/τ in conjunction with metering orifices in the blade base (ref. 6). The type of spanwise variation in τ, in conjunction with the fixed value of K, required to achieve the ideal K/τ distributions is shown in figure 5 for the three typical passages.

Figure 5 shows that the required blade shell thickness increases from root to tip. This inverse taper is undesirable with regard to stress. Figure 6 shows the strut centrifugal stresses plotted against blade span for several different tapers in shell thickness. For the blade with inverse taper, the root stress of 41,000 psi is much higher than current turbine blade practice. From stress considerations, a normal blade taper (decrease in shell thickness from root to tip) is desirable.

The attainment of the ideal permeabilities in figure 4 is inconsistent with the fabrication limitations for sintered shells and with strut centrifugal-stress limitations. For this blade design, permeability and thickness variations of the blade shell were fixed entirely from fabrication and stress-limitation considerations. To keep the strut centrifugal stress low, a normal taper from 0.050 to 0.030 inch in shell thickness from root to tip was specified. This results in a maximum strut centrifugal stress of about 30,000 psi (fig. 6), which agreed with the initial estimate. With a constant value of K this normal

taper in shell thickness results in an increase in the value of K/τ from the blade base to tip. Since this trend is opposite to that of the ideal curves of figure 4, the actual blade shell will probably be overcooled compared with the ideal blade shell.

With the spanwise variation in K/τ prescribed, the design problem becomes the determination of variation in shell temperature over the blade, amount of cooling air used, and orifice size for each passage. As noted in reference 6, the calculation of shell temperature requires iteration and is tedious. Since wall temperature T_w enters only in the flow correlation for the porous shell material (eq. (12) of ref. 6), and since its influence here is not too great (ref. 3), the tedious iteration calculation was omitted and an average value of T_w was assumed. The cooling-air flow and pressure distributions in each passage were then calculated by the method of reference 6. Boundary conditions were prescribed such that zero cooling-air flow left the passage tip, since the blade is capped, and so that the ideal cooling-air-flow rate ρv was obtained at the passage entrance (blade base). From these results the amount of cooling air used by each passage and the required orifice size for each passage were determined. The ρv values of several typical passages, obtained for the design values of shell permeability and thickness, are compared with the ideal ρv values in figure 7. For all 12 passages, the ideal ratio of total coolant flow to total gas flow is 0.020. This is increased about 65 percent to 0.033 for the design permeability.

Orifice sizes. - With a uniform cooling-air supply pressure known and the various inlet pressures at the base of each cooling-air passage available from the preceding calculations, the orifice sizes for each passage can be calculated. A cooling-air supply pressure p_a of 8352 pounds per square foot absolute (58 psia) was used. This value corresponds to compressor-discharge pressure for the design compressor pressure ratio of 4 at sea level. Values of the nozzle coefficient were taken from reference 3. Figure 8 shows the sizes of the orifices required for each coolant passage plotted against the coolant weight flow to the passage. The orifices range in size from 0.047 to 0.110 inch in diameter. Figure 8 shows that the leading- and trailing-edge passages require the largest orifices.

Fabrication Considerations

Several different ways to fabricate the strut-supported blade with a sintered shell have received consideration. Two of these will be discussed briefly. One method involves the use of an exterior mold which requires a filler in the coolant passage. The sintered powder is poured between the fins of the strut and the mold. The shell powder is then

sintered, and the whole is sintered onto the strut in a high-temperature furnace (ref. 1). The other method involves the fabrication of sheets of sintered material in the "green" state, which can be wrapped around the strut and joined to the strut along the strut fins and blade base. Each method appears to have both advantages and disadvantages; some of the difficulties that might arise with either method will now be discussed.

Use of exterior mold. - If the exterior-mold method is used, strut tolerances must be low. If these tolerances are not held to a minimum, deviations from the prescribed permeability-to-thickness variation for the shell will result. These deviations, in turn, will affect the coolant flow and the shell temperature, and blade failure could result. As a consequence, the dimensions of each cast strut will have to be individually checked (a permissible variation is ±0.002 in. in strut thickness) at various spanwise and chordwise locations. A guillotine gage is useful for such purposes. It may be possible to hold these low tolerances in production quantities; otherwise, appropriate methods must be taken to rework each strut so that the best possible blade would result.

The method of formation and attachment of the shell to the blade strut which employs the exterior mold necessitates the filling of the cooling-air passages. The filler is essential to preserve proper-sized cooling-air passages. After sintering, it must be possible to remove the filler.

Attachment of the shell at the blade base is also important. The sintering process would accomplish this attachment. Strut fillets must be large enough to avoid cracking the shell and to minimize stress concentrations. A blade cap will also be required to seal off the cooling-air passages at the blade tip, thus ensuring that the blade will be cooled solely by transpiration.

Use of sheets. - If sintered sheets are wrapped around the struts and joined along an edge to form the blade shells, the desired permeability-to-thickness ratio can be maintained even if the strut thickness tolerances are moderate (±0.005 in.). The slight alterations to the blade profile would have little, if any, effect on either coolant flow or shell temperature. This wrap-around construction method, however, would require a device that would force uniform contact of the shell to the strut fins for joining the shell to the fins.

Orifice plate. - The orifice plate can be attached to the bottom of the blade base by means of pins inserted through the base and tack-welded into position (fig. 1(a)). Centrifugal force due to rotation should provide an effective seal against loss of cooling air between the orifice plate and the lower surface of the blade base.

[redacted]

DESIGN OF WIRE-SHELL BLADE

In the experimental transpiration-cooled turbine rotor blade reported in reference 4, the porous wire cloth was wrapped around the strut and welded along the trailing edge, to the fins, to the base, and across the shell tip to form a cap. As noted in the INTRODUCTION, shell failures occurred near the blade tip along the trailing-edge weld. The necessity for a spanwise joint in the wire-cloth shell could be eliminated if the blade shell could be formed from a seamless tube and fitted over the strut. One such type of shell has been fabricated by Poroloy Equipment, Inc. (ref. 8). The blade design discussed herein could employ either type of shell.

Strut

The choice of strut material again depends on the fabrication procedure, to the extent that a satisfactory bond between the shell material and the strut material must be obtainable. S-816 alloy should again be feasible as the strut material. The stress-ratio factor for this material in the present design would again be approximately 2, assuming blade life equals that obtained in specimen pull tests.

A turbine rotor blade is subjected not only to centrifugal and thermal stresses but also to bending loads due to the fact that the centers of gravity of each spanwise section are not on a radial line. In the design for the wire-cloth blade, it was found necessary to restack the sections after the initial layouts were made in order to aline the centers of gravity on a nearly radial line.

The strut for the wire-shell blade (0.025-in. shell thickness) was designed so the outside blade profile coincided with that of the same uncooled production blade used as the basis for the design of the sintered-shell blade. Thus, this outside profile corresponds to the inside shell profile of the sintered-blade design. It was found that this requirement yields smaller strut and cooling-air-passage cross-sectional areas. Higher centrifugal stresses (35,000 psi compared with 30,000 psi) and higher cooling-air Mach numbers result.

The higher Mach numbers may result in erratic flow and pressure distributions in the cooling-air passages, as noted in reference 6. In the first strut design, there were large decreases in the passage flow areas from the blade root to tip. This resulted in erratic flow and pressure distributions inside the cooling-air passages when the ideal blade shell was calculated. Accordingly, the strut was redesigned to reduce the spanwise gradients in the passage flow areas and minimize such undesirable effects. From stress considerations, the redesign must not reduce metal area too much. In the present case, the initial design

resulted in coolant passages with excessive areas. The redesign in this case resulted simply in adding more metal to the strut. The stacking of the blade elements was not disturbed, and the erratic flow and pressure distributions in the coolant passages were eliminated. In general, however, this strut redesign may not be accomplished so easily, and compromises may be necessary.

The final strut design is shown in figure 1(c), where the layouts of three cross sections (root, mean, tip) are indicated. Again, 12 cooling-air passages are formed on each surface in addition to the leading- and trailing-edge passages. Fin widths of from 0.060 to 0.080 inch are used to provide sufficient width for attachment of the shell to the strut. The maximum unsupported width of the porous shell between strut fins is again about 0.3 inch to hold shell vibrations to a minimum. The overhang of the leading and trailing edges of the shell does not exceed 0.25 inch. As in the design of the sintered-shell blade, the shell vibration problems at the blade leading and trailing edges were not considered.

Typical passage geometries for the wire-cloth blade, measured from scaled layouts of strut cross sections, are given in table II. Note that nearly linear spanwise variations in passage flow area are used. The design of the blade base is essentially the same as for the sintered blade.

3990

Shell

The shell for the wire blade is designed for conditions comparable with those used for the design of the sintered shell. The appropriate theories of reference 6 were again employed. A typical shell material might be stainless-steel wire cloth.

Distribution of gas pressure and velocity. - Chordwise variations in gas static pressure and gas velocity relative to the blade were determined at three spanwise locations (fig. 9). An estimate of the transition points from laminar to turbulent flow on the blade surfaces is made in the same manner as discussed previously, and again passages 1 to 5 are found to be in the laminar gas-flow region and passages 6 to 12 in the turbulent gas-flow region.

Variation of ideal coolant flow and permeability-to-thickness ratio. - An effective gas temperature T_g of 1425° F is again used. The same linear spanwise variation in cooling-air temperature as used in the sintered-blade design (i.e., $T_c = 180 + 644x$ °F) is assumed. A shell temperature T_w of 600° F is prescribed, for the same reasons as given previously. Spanwise variations in ideal cooling-air flow ρv are then calculated for each passage, using the appropriate laminar or turbulent heat-transfer theory. Examples of these variations are shown in figure 10(a).

[redacted]

The spanwise variation in gas pressure is found from the data of figure 9, and examples are given in figure 10(b). The geometry of the cooling-air passages necessary for the calculation of the cooling-air pressure p_i is given in table II. The spanwise variation in cooling-air pressure is calculated for each passage, and the results for typical passages are shown in figure 10(c). Finally, the ideal spanwise variation in the permeability-to-thickness ratio K/τ is calculated for each passage, by substituting $T_w = 1060^\circ$ R (600° F) into the flow correlation for wire cloth given by equation (12) of reference 6 and solving for K/τ. The result is

$$\frac{K}{\tau} = 0.00356 \frac{(\rho v)^{1.6}}{p_i^2 - p_e^2} \tag{4}$$

The ideal spanwise variations in K/τ for the 12 cooling-air passages of this blade design are given in figure 11.

Compromises in permeability-to-thickness ratio. - Figure 11 shows that wide chordwise and spanwise variations in K/τ are required to maintain the prescribed shell temperature. These permeability variations are extremely difficult, if possible, to obtain. Compromises are therefore necessary. Use of a constant chordwise permeability in conjunction with orifices in the blade base to meter the cooling air to each blade passage partially compensates for a constant chordwise K/τ. The compromise spanwise variation must be obtained from a consideration of the ideal curves in figure 11 and from the type of permeability variation that can be fabricated. Several permeabilities for the blade shell have been considered. These are discussed in the following paragraphs.

From the ideal spanwise permeability distributions calculated for the 12 coolant passages (fig. 11), shell permeabilities feasible with respect to fabrication and such that the porous wall temperature nowhere exceeds the design value of 600° F may be employed. For each permeability the amount of cooling air used in each passage was estimated by using the short-form solution for the internal coolant pressure p_i as indicated in reference 6, and eliminating the tedious iteration process by assuming an average value of wall temperature. From the estimated cooling-air consumption for these passages, an estimate of the amount of cooling air used by the entire blade was available. Four different specifications were considered.

Case 1: For case 1, a constant chordwise and constant spanwise shell permeability-to-thickness ratio K/τ equal to the maximum ideal values calculated for the passages, $K/\tau = 0.60 \times 10^{-9}$ foot, was used.

Case 2: For case 2, constant chordwise but different constant spanwise values of K/τ were used for the suction surface and pressure

surface of the blade, equal in each case to the maximum ideal value calculated for the passages on the blade surface. (The leading-edge passage was considered to be on the pressure surface; the trailing-edge passage, on the suction surface.) For the pressure surface, $K/\tau = 0.60\times10^{-9}$ foot; for the suction surface, $K/\tau = 0.22\times10^{-9}$ foot.

Case 3: For case 3, constant chordwise and variable spanwise values of K/τ with the same spanwise variation on both pressure and suction surfaces were used. This spanwise variation was chosen as the envelope of the ideal spanwise variations and is shown in figure 12(a).

Case 4: For case 4, a constant chordwise value of K/τ but different spanwise variations in K/τ for the pressure and suction surfaces were used. These spanwise variations were chosen as the envelopes of the ideal spanwise variations calculated for each surface and are shown in figure 12(b).

From the results of these calculations, the total weight flow of cooling air w_{to} for the turbine rotor was found for each case, assuming a fully cooled wheel with 54 cooled blades. The ratio of w_{to} to the engine gas weight flow was calculated for an engine gas flow of 75 pounds per second. Finally, the ratio of design total cooling-air flow to the ideal total cooling-air flow was calculated in each case. These results are tabulated as follows:

Case	$\frac{w_{to}}{\text{Engine gas weight flow}}$	$\frac{\text{Design cooling-air consumption}}{\text{Ideal cooling-air consumption}}$
Ideal	0.020	1.0
1	.065	3.3
2	.047	2.4
3	.037	1.9
4	.029	1.5

This table shows that case 4, the specified variable spanwise K/τ with a different variation specified for each blade surface, is to be preferred, since the excess cooling-air flow is only about 50 percent. The case of a constant permeability over the entire blade surface, case 1, is undesirable, since there is an excess flow of cooling air of 230 percent over the ideal flow. A good convection-cooled blade (impermeable shell) would probably be more effective than a transpiration-cooled blade with case 1 permeability. Cases 2 and 3 are intermediate, the excess coolant flow being about 140 percent and 90 percent, respectively, over the ideal value. From these figures it is apparent that the potential of transpiration cooling of turbine rotor blades, with the low amounts of cooling air ideally required, must be compromised to allow for a blade shell that is feasible with regard to present fabrication methods.

Orifice sizes. - The orifice sizes for the three typical blade passages (1, 4, and 10) were calculated. The cooling-air supply pressure at the blade base p_a was again assumed to be 8352 pounds per square foot absolute (58 psia). A typical value of the nozzle coefficient, determined experimentally in reference 3, was taken as 0.84 in all cases. The results for the three passages are presented in the following table:

Case	Orifice diameter, in.		
	Leading-edge passage 1	Midchord suction-surface passage 4	Midchord pressure-surface passage 10
Ideal	0.097	0.024	0.045
1	.144	.070	.062
2	.144	.052	.062
3	.111	.054	.047
4	.111	.042	.047

These diameters are of the same order of magnitude as in figure 8 for the sintered blade.

Fabrication Considerations

The attachment of the wire shell to the strut fins is a major problem. In the blades of reference 4, the wire cloth was welded to the strut fins, and numerous dimples over the blade profile resulted. To eliminate this undesirable effect, fabricators, in initial attachment attempts, might resort to brazing. As is the case with the sintered blade, some exterior device will be required to ensure good contact between shell and strut fins. Moderate strut tolerances of the order of those for the wrap-around sintered blades should be permissible.

Attachment of the shell to the blade base will be necessary to prevent cooling-air leakage. The blade cap may be achieved by forming an elongated shell and joining the shell halves at the blade tip. (This was done to the blades reported in ref. 4.) The orifice plate may be attached at the blade base by means of pins tack-welded to the base, as in the sintered-blade design. Centrifugal force due to rotation should again provide an effective seal against loss of cooling air at the blade base.

GENERAL COMMENTS

Because the same standard engine conditions were chosen for both the sintered-shell and the wire-shell blades, there are no great differences in blade shape. As was already noted, however, the strut for the wire-shell blade is thinner than that for the sintered-shell blade. The

lesser metal area for the wire-shell blade resulted, therefore, in a higher maximum centrifugal stress (35,000 psi) than for the sintered-shell blade (30,000 psi). In the stress calculations for both blades, no credit was given to the shell for any load-carrying ability. As noted in reference 9, however, wire cloths appear much stronger than sintered materials. It would be logical to expect, therefore, that the wire shell may carry more of its centrifugal load than the sintered shell. This would result in closer agreement in the maximum strut centrifugal stress (i.e., reduce the 35,000-psi figure).

The ideal total coolant- to total gas-flow ratio is about 0.02 for both the sintered-shell and the wire-shell blades. Hence, there is little to choose between the two blade designs in the ideal case. In comparing the two blades for the design cases, the conditions for which the respective calculations were made must be kept clearly in mind. Such comparisons will only serve to indicate trends. Specification of design variations in shell permeabilities were made from different considerations for the two blades. These are reviewed in the following paragraphs.

When the ideal requirements for the sintered-shell blade were found, there was no experience available in the fabrication of shells of variable permeability-to-thickness ratio. The simplest approach appeared to be holding a constant permeability and varying the thickness. Unfortunately, this resulted in inverse taper, which is precluded from stress considerations. To minimize overcooling, the lowest possible value of permeability K was desired. The value of K selected (8×10^{-10} sq in.) was the smallest value that could be fabricated with adequate control of random variations. From strut stress considerations, a normal taper in shell thickness of 0.050 to 0.030 inch was chosen.

For the wire-shell blade, design permeability approaching ideal values was considered. The attainment of such permeabilities may be more feasible for wire shells than for sintered shells. To explore these possibilities further, four different permeability variations were considered. The variation most closely approaching the ideal was found to be a constant chordwise value of K/τ but different spanwise variations for the pressure and suction blade surfaces. The case most easily fabricated was for a constant permeability both chordwise and spanwise. For this case, the values chosen were $K = 1.8\times10^{-10}$ square inch, and $\tau = 0.025$ inch.

The preceding discussions indicate in which directions the fabricators of porous materials must concentrate their efforts in order to produce the type of porous blade shell ultimately desired. On the basis of present knowledge and the calculations reported herein, it is apparent that lower permeabilities with adequate control of random variations in permeability, spanwise variations in permeability, and reduced blade shell thicknesses appear desirable for sintered-shell blades. On the same basis, it appears more desirable to achieve spanwise variations in permeability for wire-cloth shells than for sintered shells.

The attachment of the shell to the strut introduces complications for both types of shells. From the view of improving allowable strut tolerances, it appears advisable to use a wrap-around technique. Even so, some means of assuring contact between strut and shell at the junction areas must be provided. Although in the wrap-around technique used in reference 4 the shell was at room temperature, it may be necessary to treat the shell to increase its pliability (e.g., by heating). Such action would depend not only on the type of shell used, but also on its permeability and thickness.

Insofar as the relative ease of fabrication of the two blades and their durability in engine operation are concerned, no general statement can now be made. Although the results of reference 4 give some indication of the feasibility of wire cloth for the present application, additional experimental work in fabrication and testing of both types of blades is needed before general conclusions can be reached.

SUMMARY OF RESULTS

The design details of two transpiration-cooled turbine rotor blades have been presented. One blade used a porous shell of sintered powder and the other a wire-cloth shell; both blades were strut-supported. Ideal coolant flows were found for an effective gas temperature of 1425° F, a coolant temperature of 180° F, and a shell temperature of 600° F. Although these temperatures prevail in a test vehicle, approximately the same coolant flow will obtain in a high-temperature application. The principal results are summarized as follows:

1. For the foregoing conditions, the ideal permeability-to-thickness variations that result appear difficult to fabricate for both sintered and wire blades. For the blade with a sintered shell, use of presently available permeabilities resulted in shell thickness variations that made centrifugal stresses prohibitive.

2. For the permeability-to-thickness compromises investigated, the blade with the sintered shell required about 1.65 times as much cooling-air flow as the ideal requirement; the blade with the wire shell required from 1.5 to 3.3 times as much coolant, depending on the compromise. These compromises result in cooling the shell below the specified temperature of 600° F.

3. Selection of strut material depends on imposed stresses and shell attachment and fabrication methods. Strut redesign may be necessary to eliminate erratic spanwise variations in cooling-air pressure as well as to minimize centrifugal and bending stresses.

4. For design conditions the orifices range in size from 0.047 inch to 0.110 inch in diameter for the sintered blade. Comparable sizes are indicated for the blade with the wire shell. In both instances, the leading- and trailing-edge passages require the largest orifices.

Lewis Flight Propulsion Laboratory
National Advisory Committee for Aeronautics
Cleveland, Ohio, January 30, 1956

REFERENCES

1. Bartoo, Edward R., Schafer, Louis J., Jr., and Richards, Hadley T.: Experimental Investigation of Coolant-Flow Characteristics of a Sintered Porous Turbine Blade. NACA RM E51K02, 1952.

2. Schafer, Louis J., Jr., Bartoo, Edward R., and Richards, Hadley T.: Experimental Investigation of the Heat-Transfer Characteristics of an Air-Cooled Sintered Porous Turbine Blade. NACA RM E51K08, 1952.

3. Esgar, Jack B., and Richards, Hadley T.: Evaluation of Effects of Random Permeability Variations on Transpiration-Cooled Surfaces. NACA RM E53G16, 1953.

4. Donoughe, Patrick L., and Diaguila, Anthony J.: Exploratory Engine Test of Transpiration-Cooled Turbine-Rotor Blade with Wire-Cloth Shell. NACA RM E53K27, 1954.

5. Eckert, E. R. G., Livingood, John N. B., and Prasse, Ernst I.: One-Dimensional Calculation of Flow in a Rotating Passage with Ejection through a Porous Wall. NACA TN 3408, 1955.

6. Prasse, Ernst I., and Livingood, John N. B.: Design Procedure for Transpiration-Cooled Strut-Supported Turbine Rotor Blades. NACA RM E55J21, 1955.

7. Probst, Robert L.: Investigation of Sintered Loose Spherical Powder for Fabrication into Transpiration Cooled Turbine Blades. Final Rep., Federal-Mogul Corp., July 1955. (Bur. Aero., U. S. Navy Dept. Contract NO as 51-613-C.)

8. Anon.: Introducing a New Porous Metal - Poroloy. Poroloy Equipment, Inc., Pacoima (Calif.).

9. Donoughe, Patrick L., and McKinnon, Roy A.: Experimental Investigation of Air-Flow Uniformity and Pressure Level on Wire Cloth for Transpiration-Cooling Applications. NACA TN 3652, 1956. (Supersedes NACA RM E52E16.)

[redacted]

TABLE I. - TYPICAL PASSAGE GEOMETRY FOR SINTERED BLADE

[Coolant-passage length L, 0.325 ft.]

Passage number	Distance from base, x, ft	Passage flow area, A, sq ft	Passage width, b, ft	Passage hydraulic diameter, D_h, ft
1	0.021	2.25×10^{-4}	0.045	0.0144
	.093	1.74	.038	.0123
	.165	1.24	.031	.0101
	.237	.74	.024	.0080
	.310	.24	.016	.0058
4	0.021	0.69×10^{-4}	0.021	0.0062
	.093	.73	.021	.0064
	.165	.78	.022	.0066
	.237	.82	.022	.0068
	.310	.86	.023	.0070
10	0.021	0.69×10^{-4}	0.021	0.0059
	.093	.73	.021	.0060
	.165	.76	.021	.0062
	.237	.80	.022	.0063
	.310	.83	.023	.0065

TABLE II. - TYPICAL PASSAGE GEOMETRY FOR WIRE-CLOTH BLADE

[Coolant-passage length L, 0.325 ft.]

Passage number	Distance from base, x, ft	Passage flow area, A, sq ft	Passage width, b, ft	Passage hydraulic diameter, D_h, ft
1	0.026	1.243×10^{-4}	0.0349	0.01027
	.096	.980	.0365	.00836
	.176	.667	.0344	.00632
	.256	.368	.0323	.00403
	.296	.208	.0187	.00389
4	0.026	0.653×10^{-4}	0.0193	0.00619
	.096	.514	.0177	.00540
	.176	.375	.0167	.00424
	.256	.208	.0148	.00271
	.296	.132	.0144	.00180
10	0.026	0.854×10^{-4}	0.0193	0.00728
	.096	.674	.0182	.00624
	.176	.444	.0172	.00449
	.256	.236	.0151	.00295
	.296	.125	.0144	.00166

[redacted]

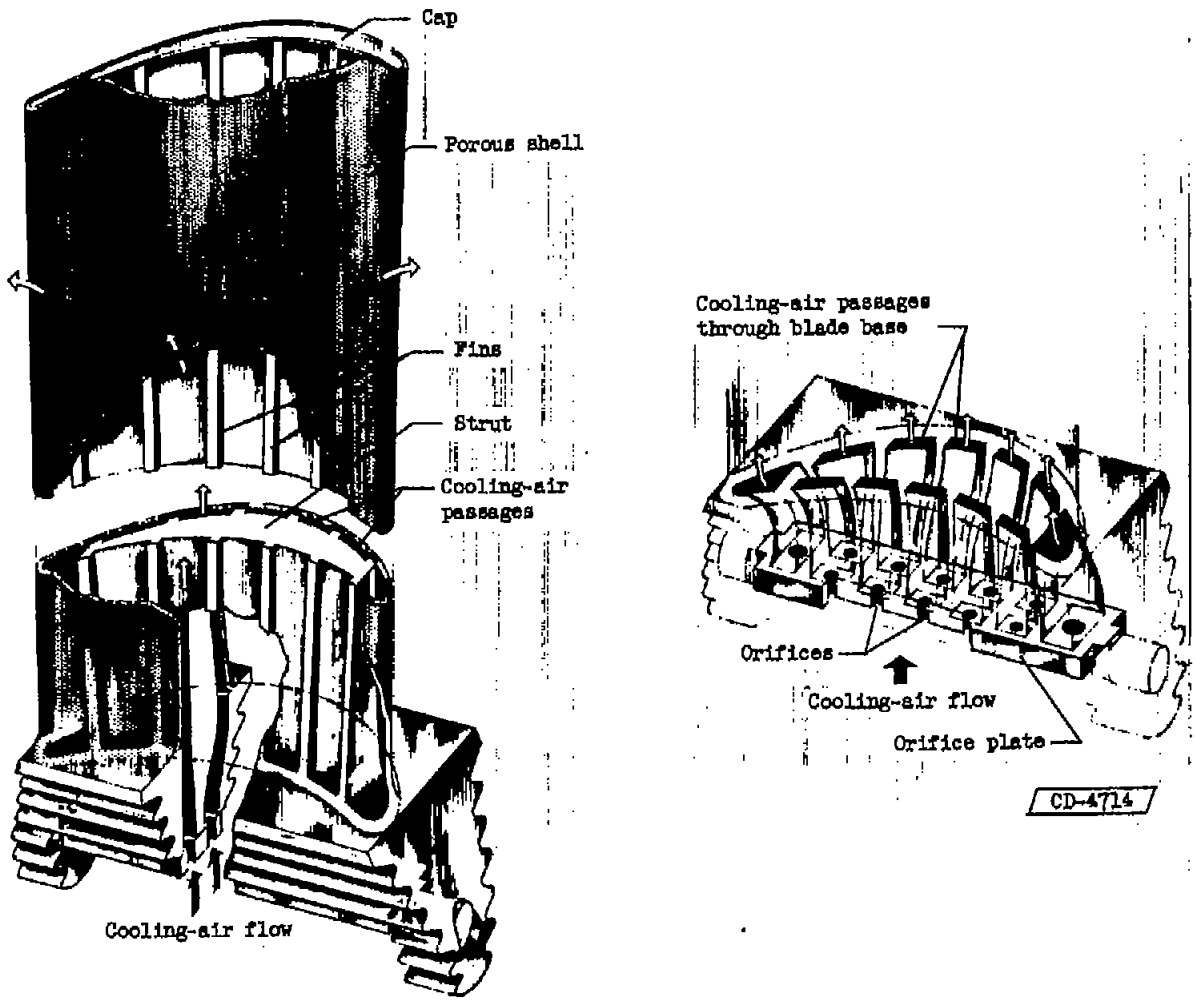

(a) Transpiration-cooled strut-supported turbine rotor blade.

Figure 1. - Transpiration-cooled strut-supported turbine rotor blade, and layouts of strut cross sections for sintered-shell and wire-shell blades.

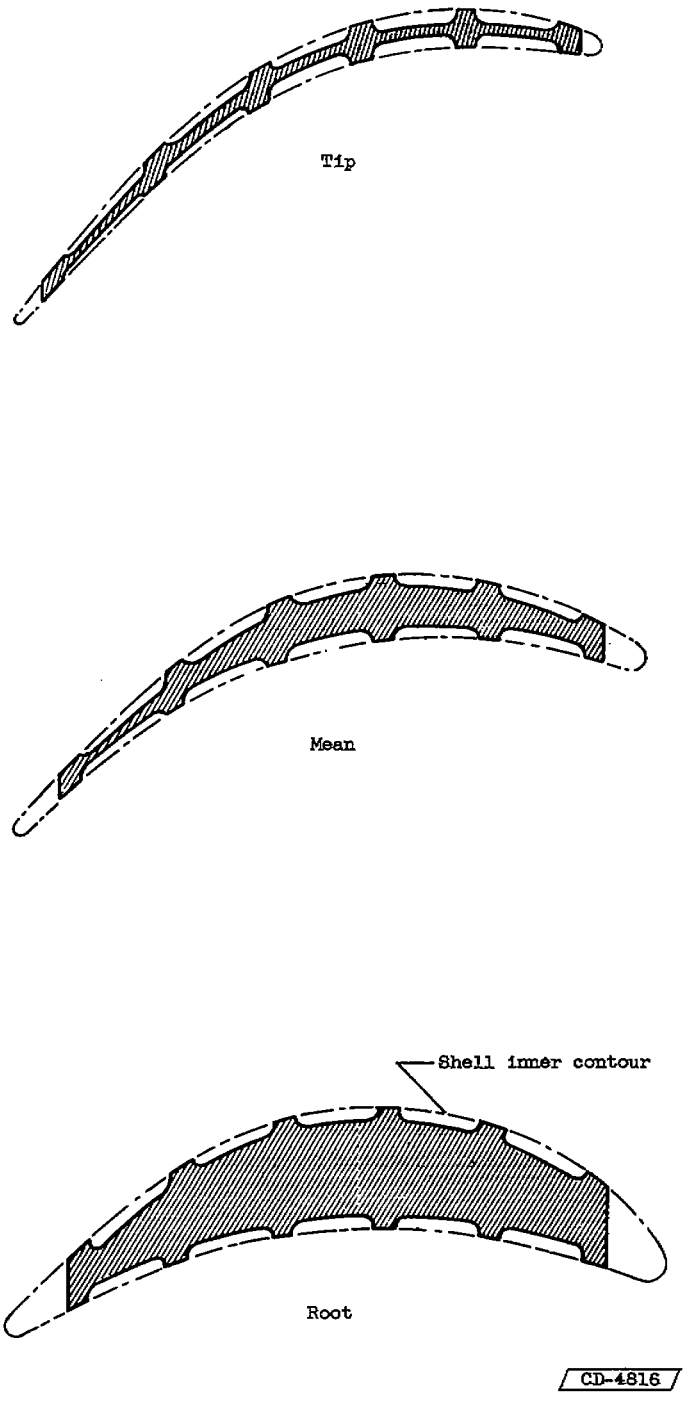

(b) Strut cross sections of sintered-shell blade.

Figure 1. - Continued. Transpiration-cooled strut-supported turbine rotor blade, and layouts of strut cross sections for sintered-shell and wire-shell blades.

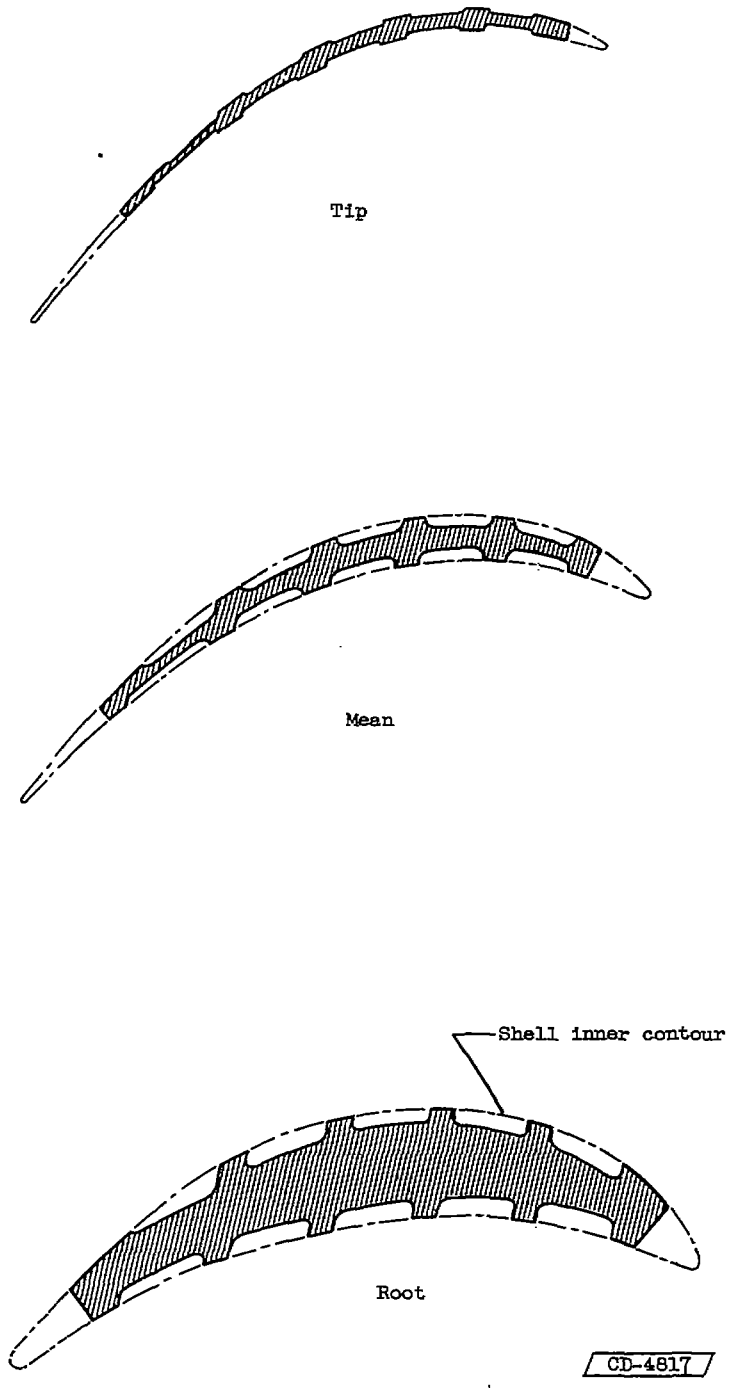

(c) Strut cross sections of wire-shell blade.

Figure 1. - Concluded. Transpiration-cooled strut-supported turbine rotor blade, and layouts of strut cross sections for sintered-shell and wire-shell blades.

[redacted]

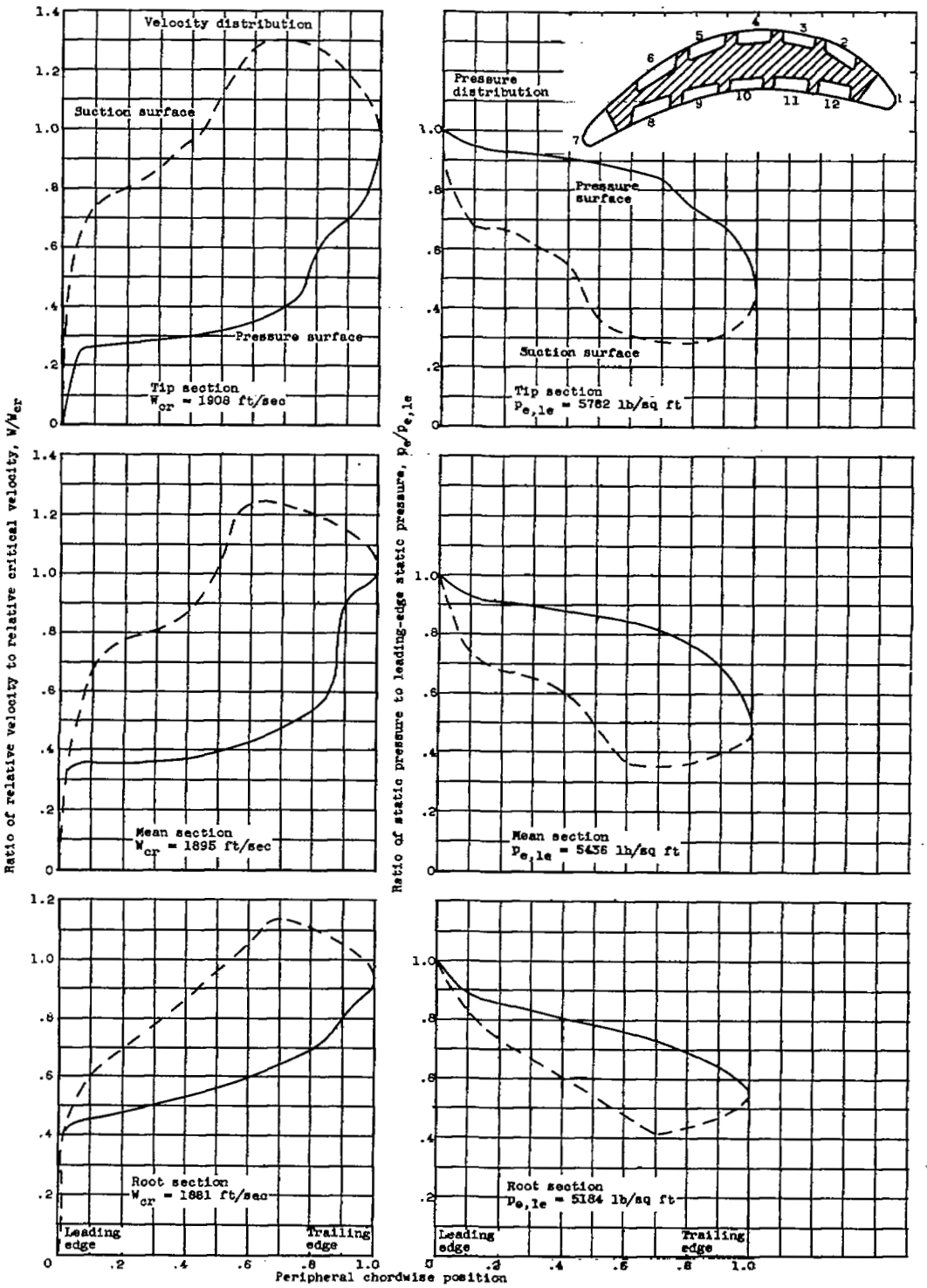

Figure 2. - Chordwise variations of relative gas velocity and gas pressure for sintered-shell blade.

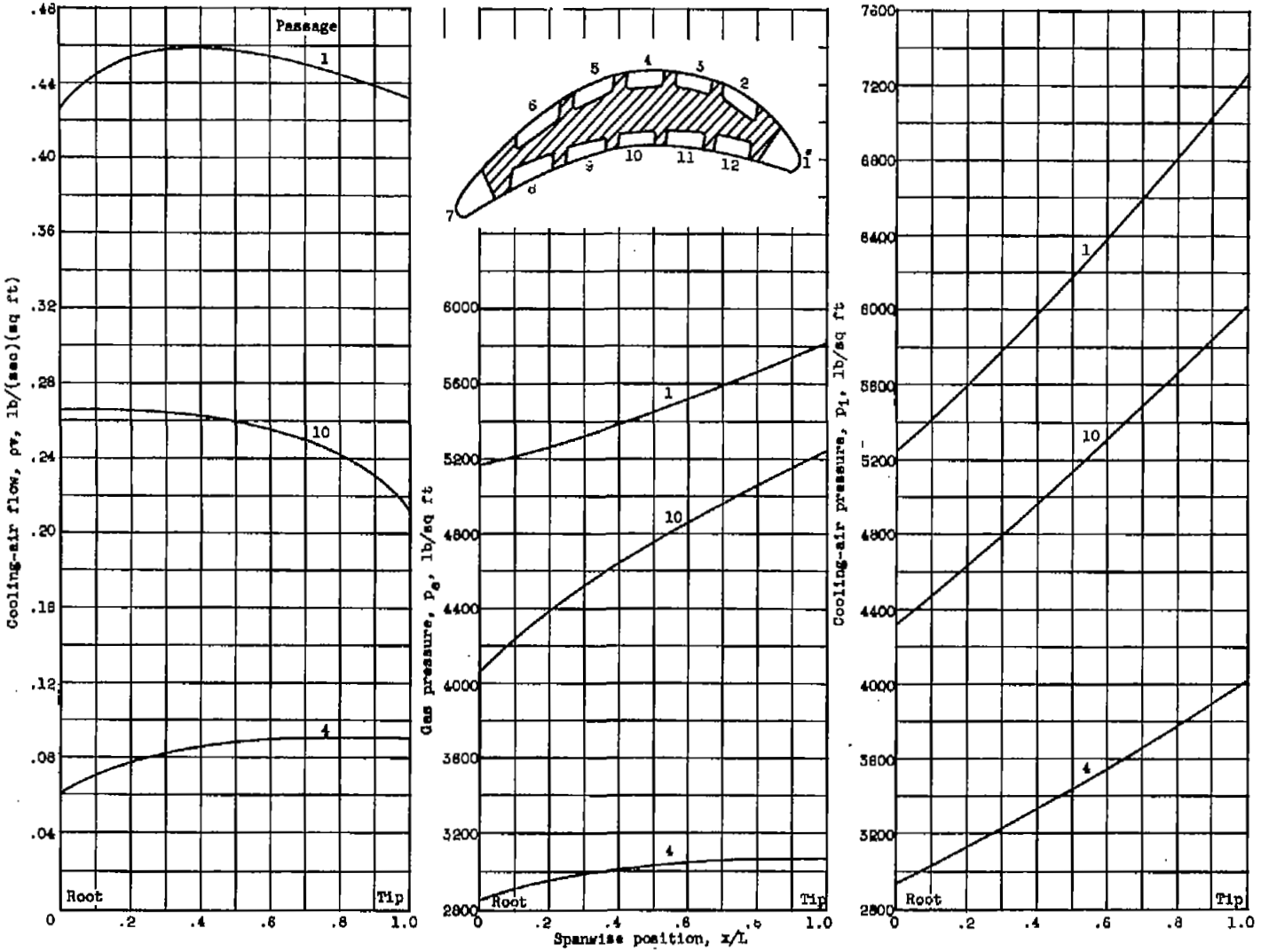

(a) Ideal cooling-air flow. (b) Gas pressure. (c) Cooling-air pressure.

Figure 3. - Typical examples of spanwise variations in ideal cooling-air flow, gas pressure, and cooling-air pressure for passages 1, 4, and 10 of sintered-shell blade.

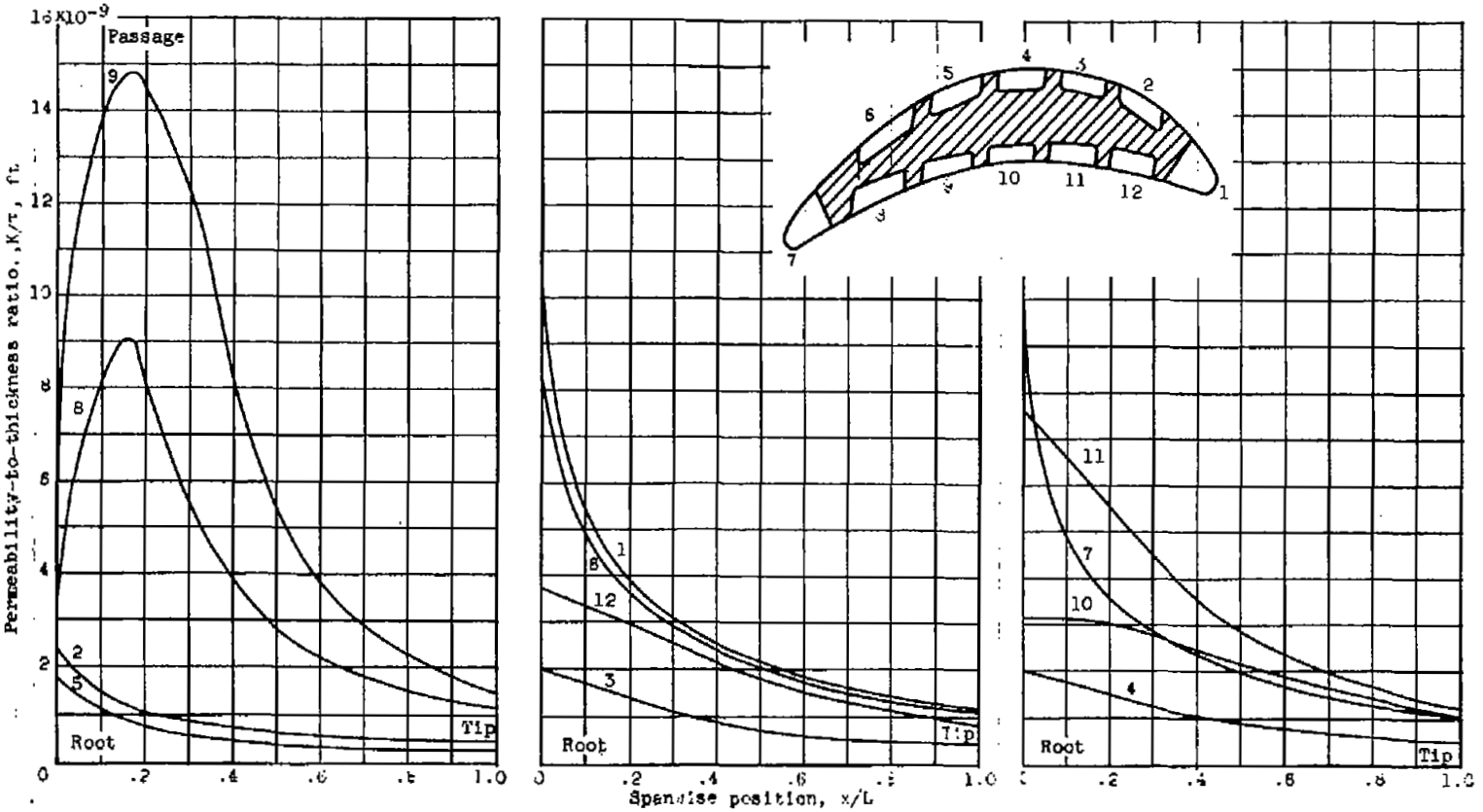

Figure 4. - Ideal spanwise variations in shell permeability-to-thickness ratio for passages of sintered-shell blade.

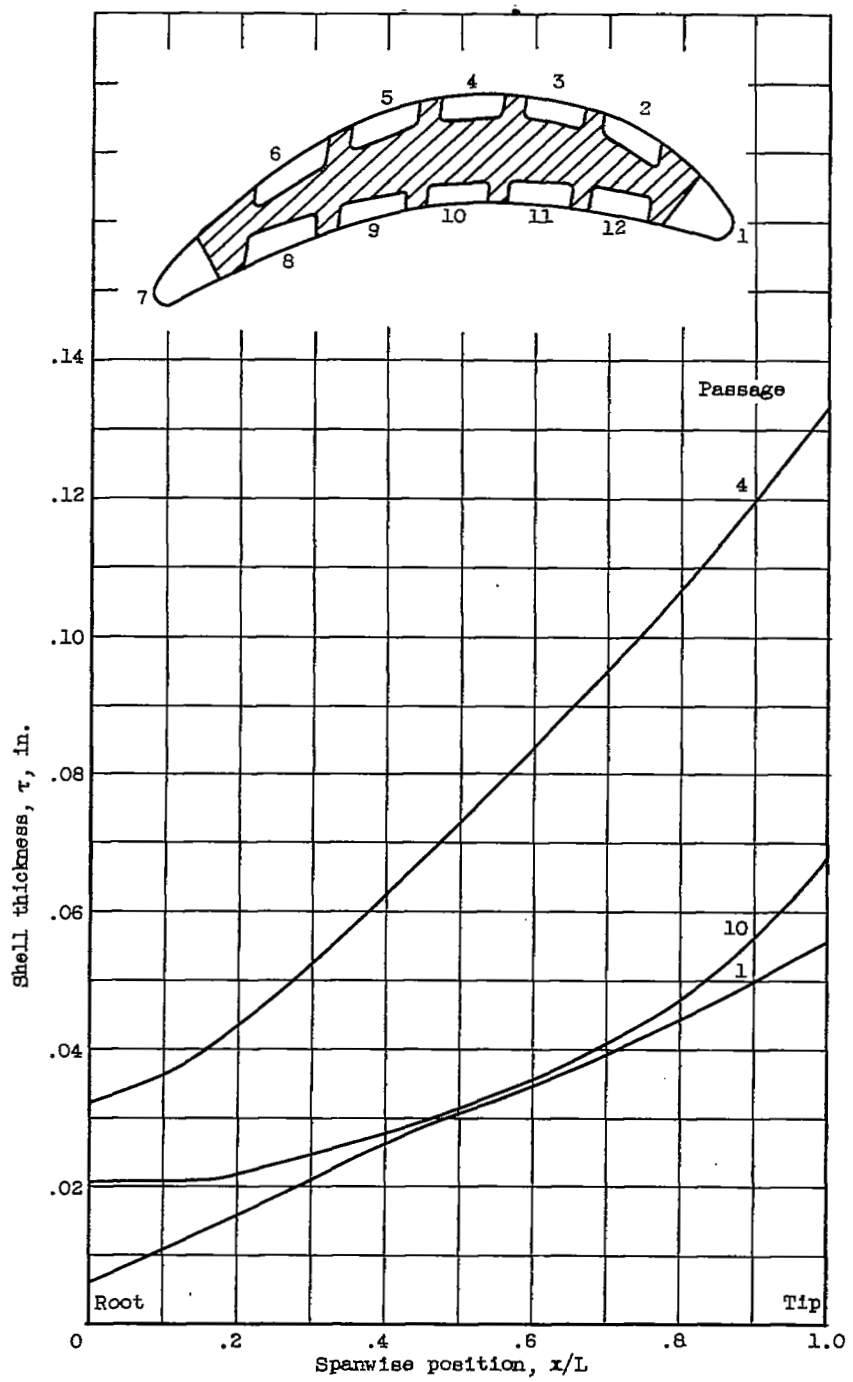

Figure 5. - Typical required spanwise variation in shell thickness to obtain ideal variation in shell permeability-to-thickness ratio with constant shell permeability of 8×10^{-10} square inches.

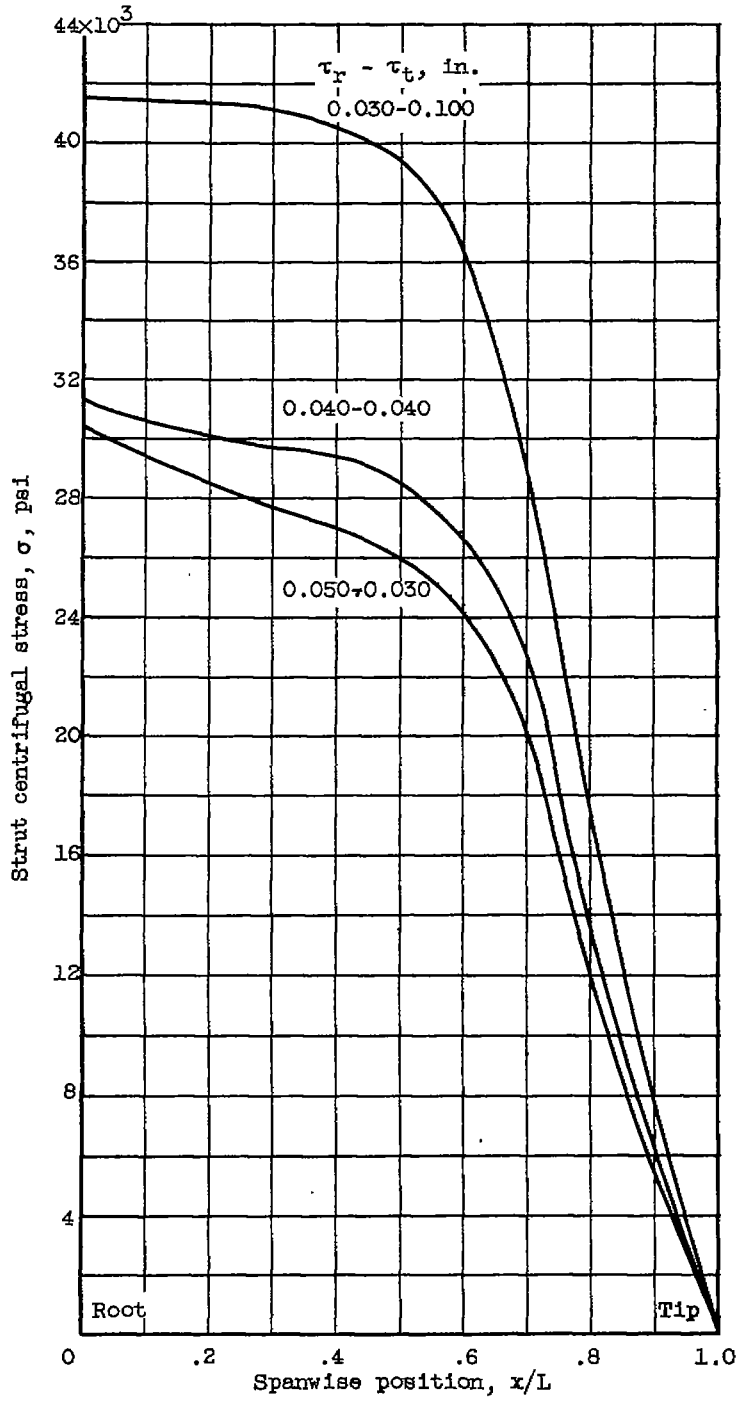

Figure 6. - Effect of spanwise taper in shell thickness on strut centrifugal stresses for sintered-shell blade.

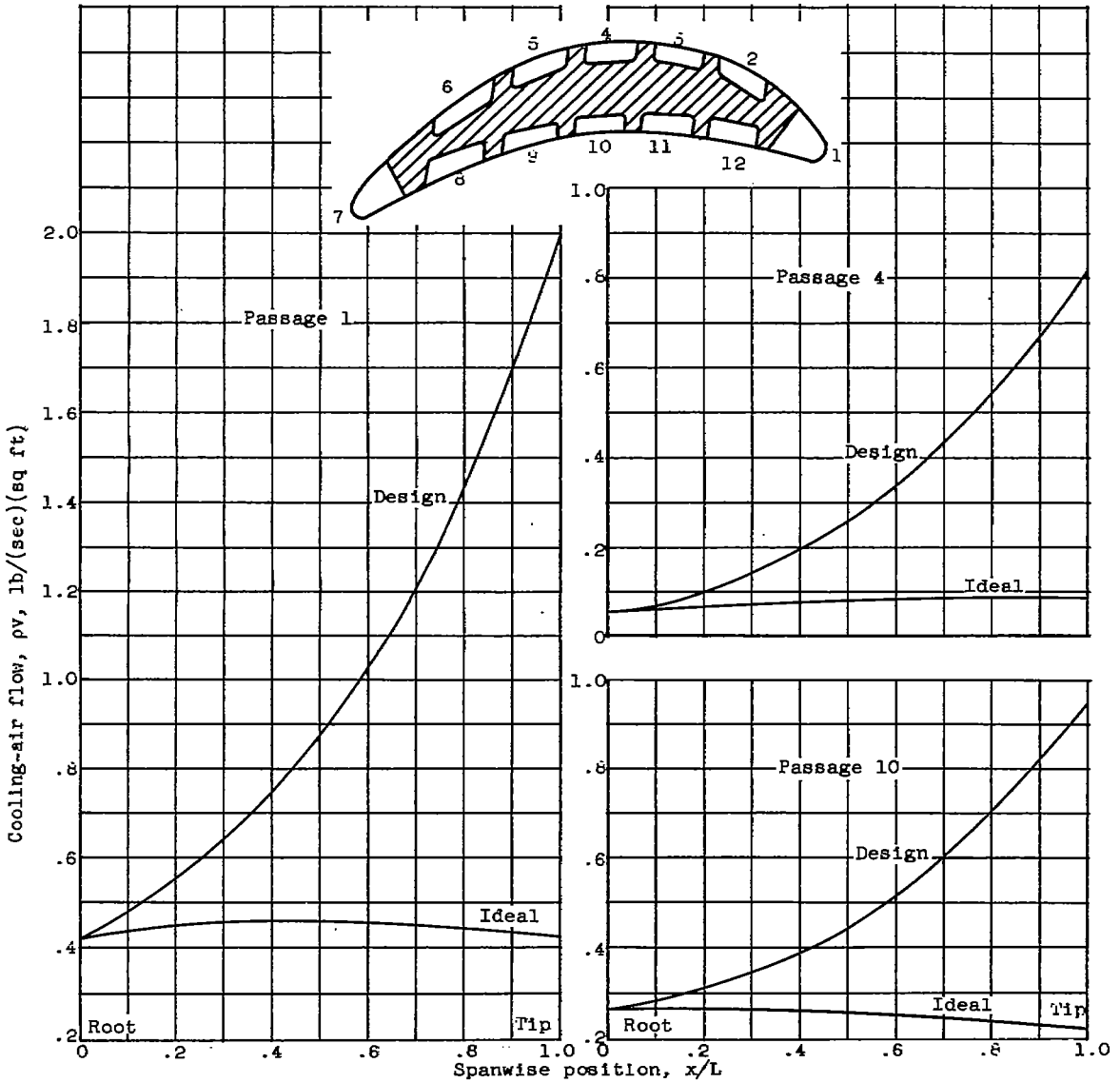

Figure 7. - Comparison of ideal and design cooling-air flow for typical passages of sintered-shell blade.

[redacted]

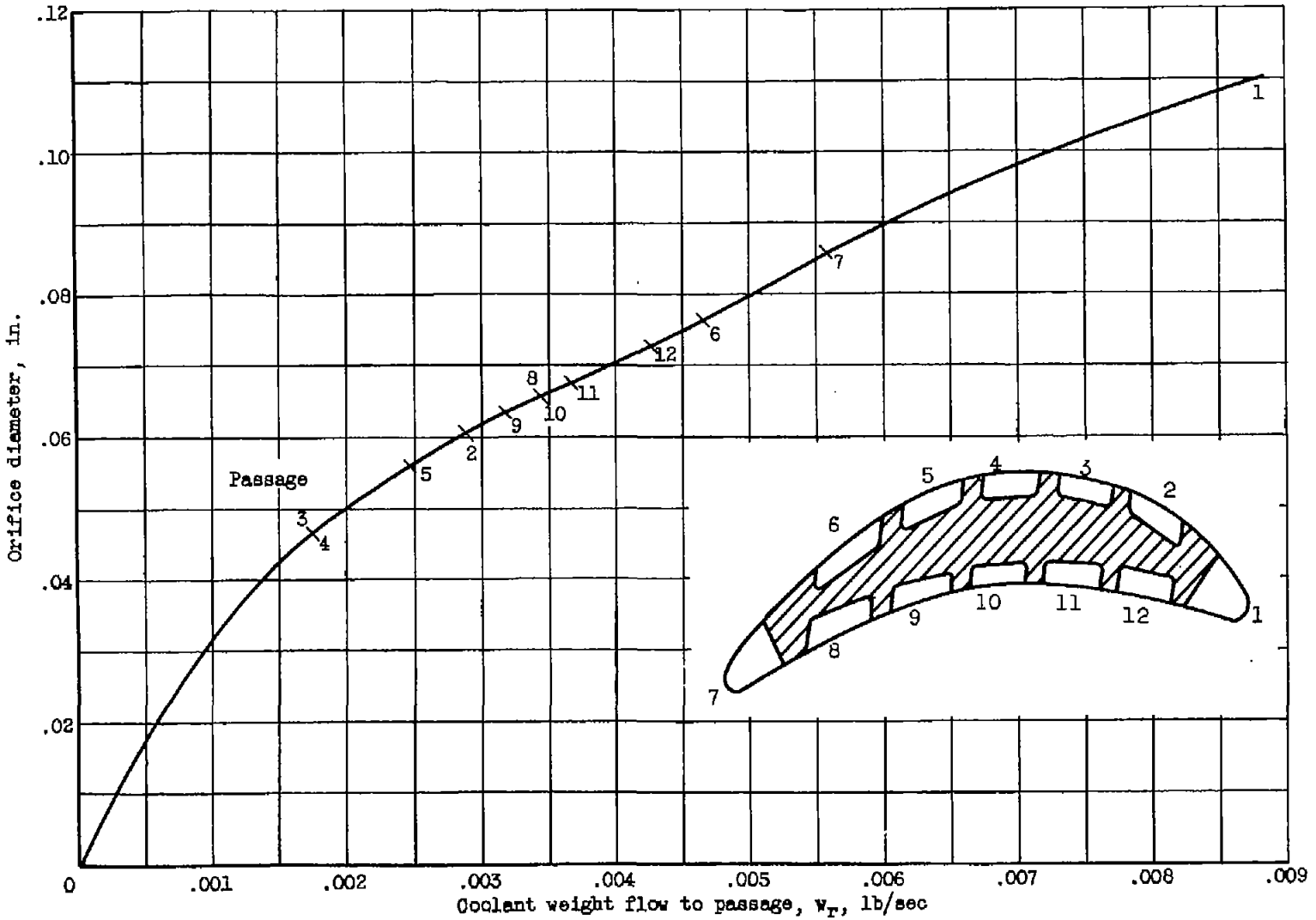

Figure 8. - Design orifice sizes for passages of sintered-shell blade.

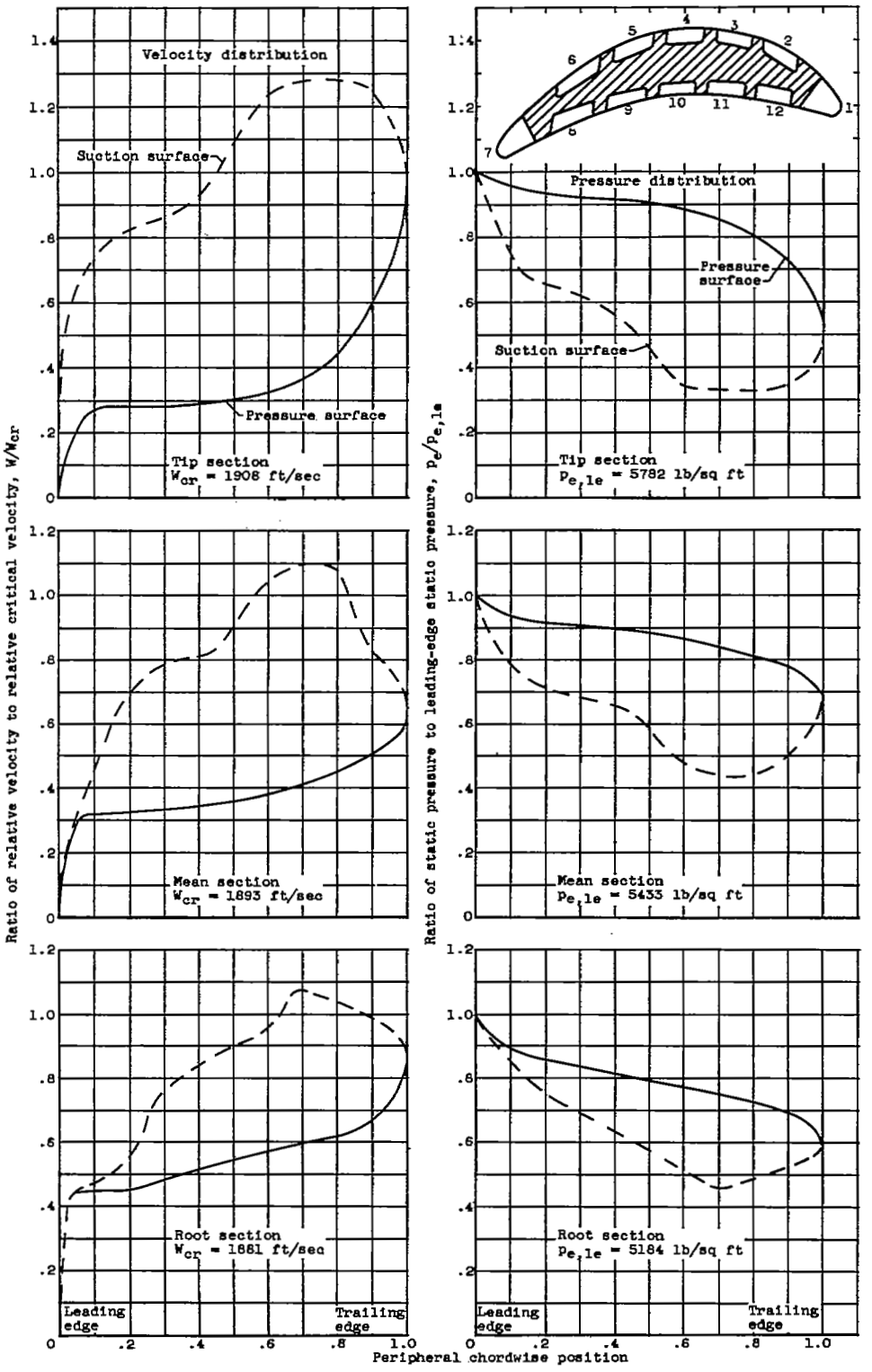

Figure 9. - Chordwise variations of relative gas velocity and gas pressure for wire-shell blade.

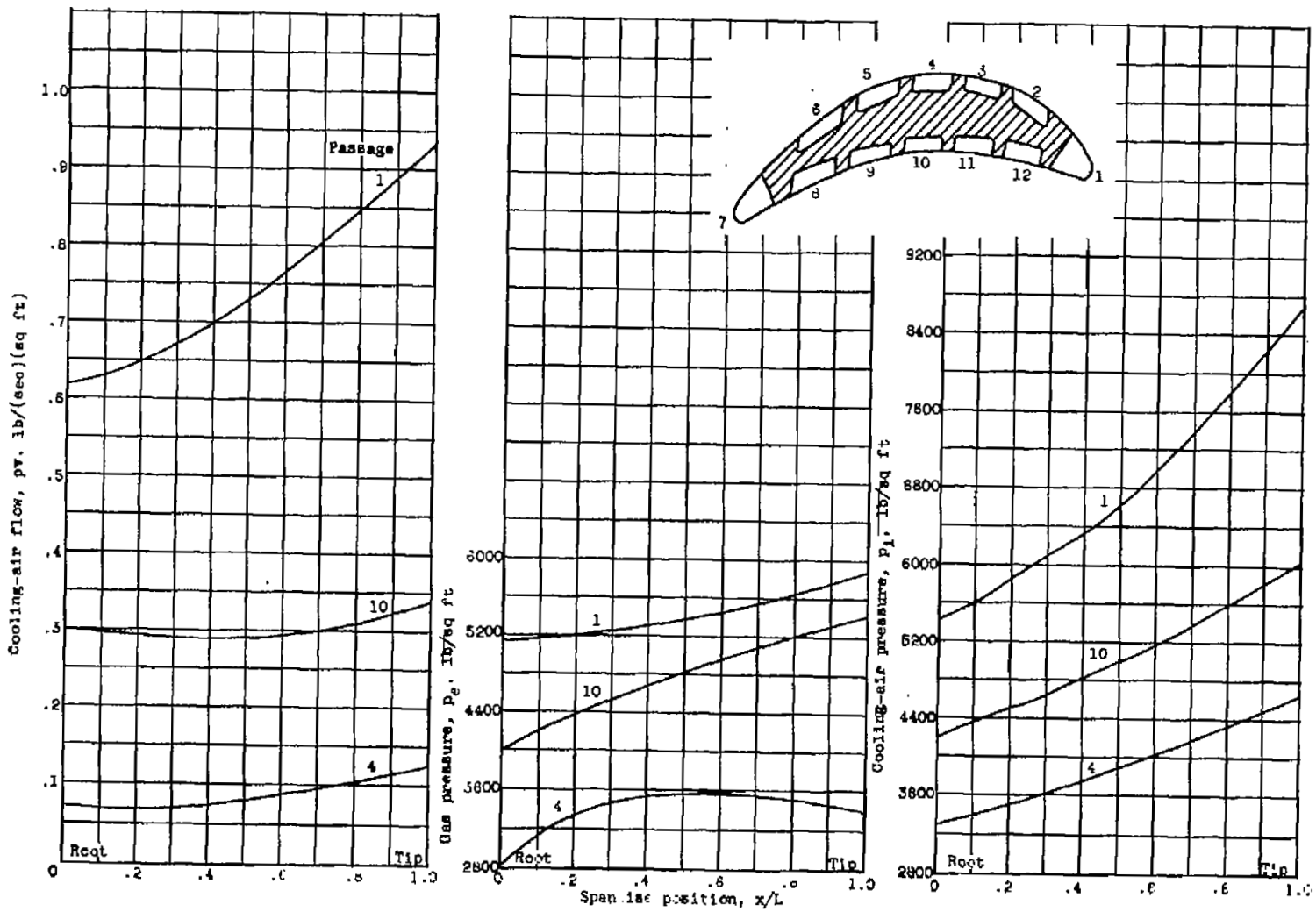

(a) Ideal cooling-air flow. (b) Gas pressure. (c) Cooling-air pressure.

Figure 10. - Typical examples of spanwise variations in ideal cooling-air flow, gas pressure, and cooling-air pressure for passages of wire-shell blade.

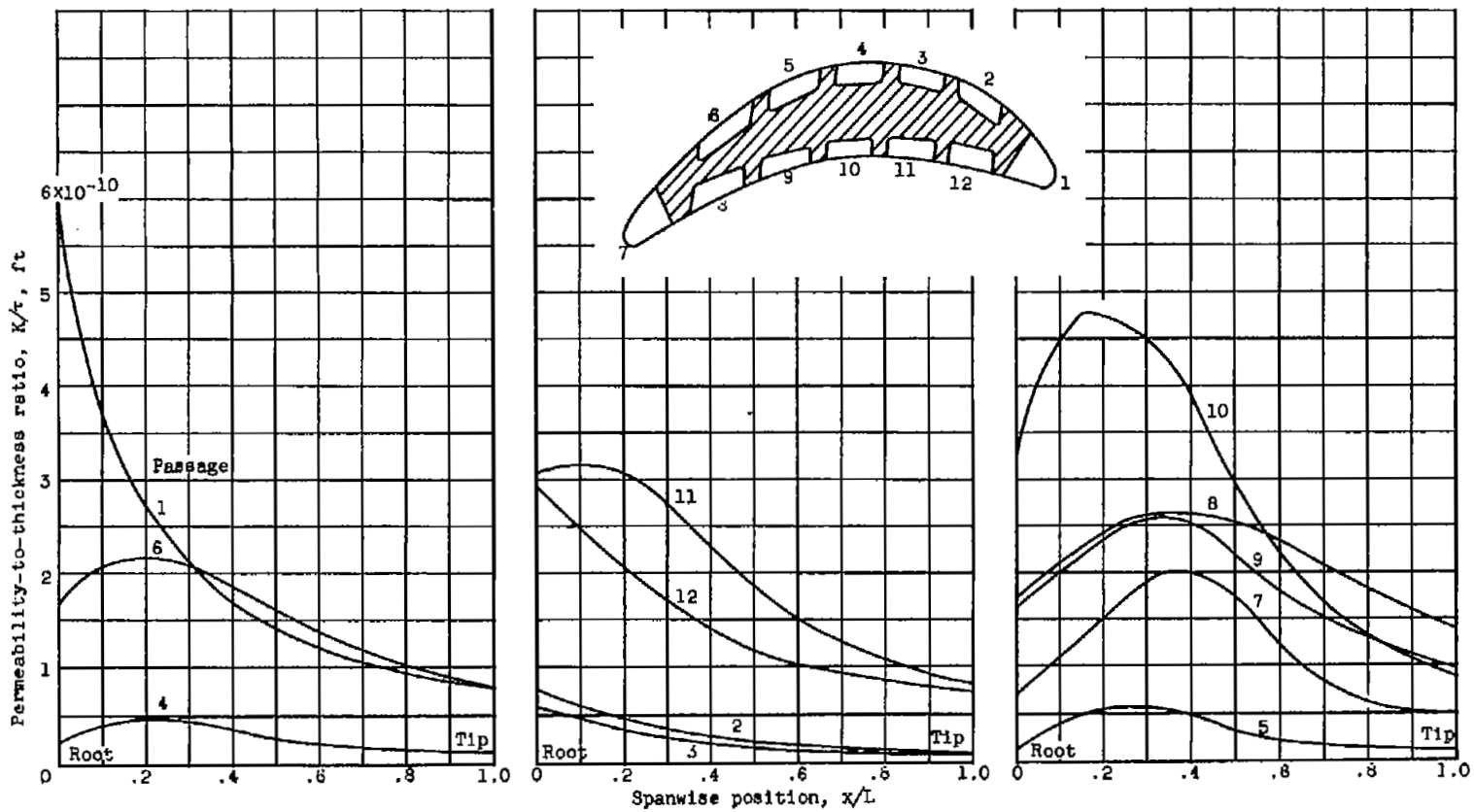

Figure 11. - Ideal spanwise variations in shell permeability-to-thickness ratio for passages of wire-shell blade.

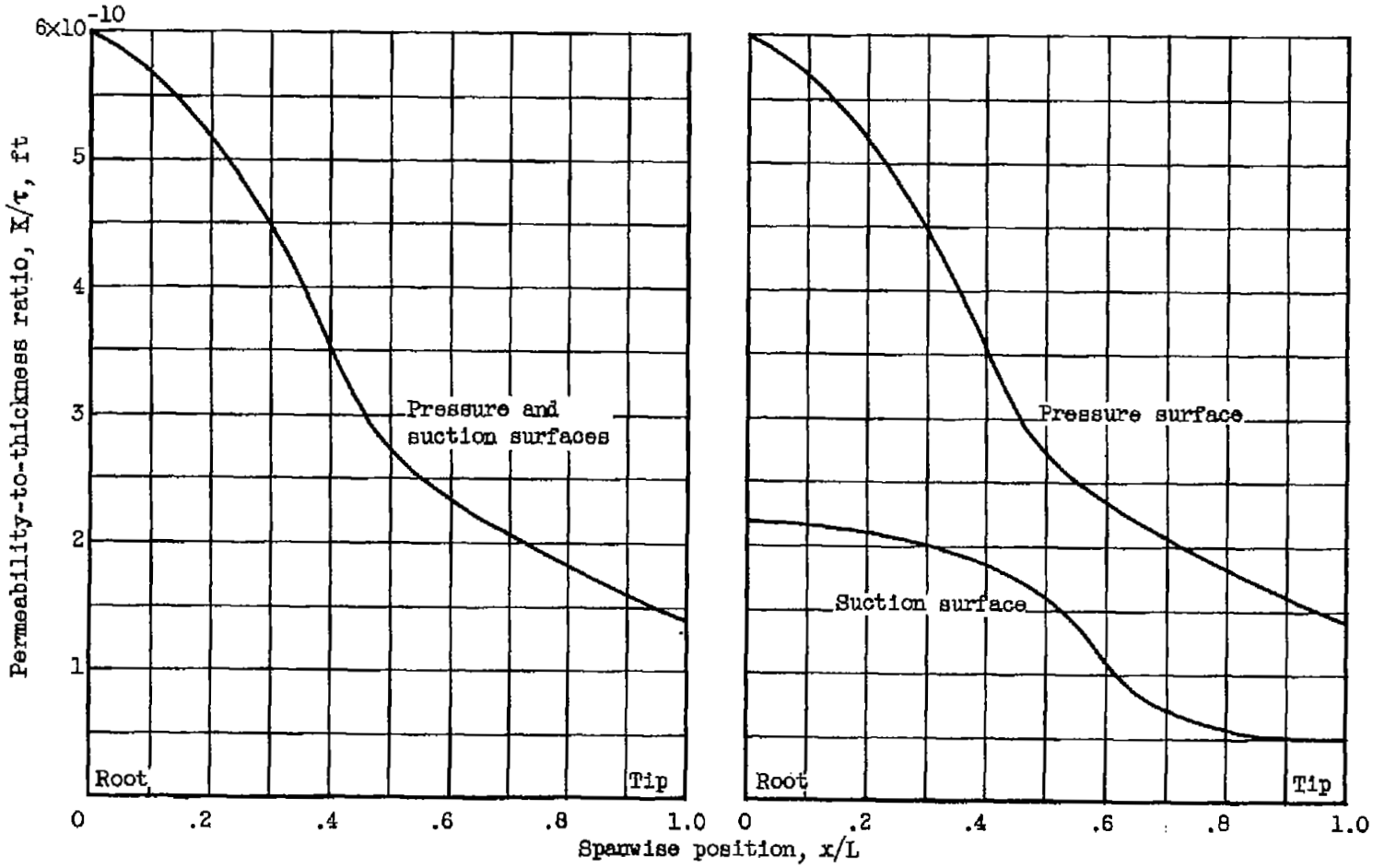

(a) Case 3.

(b) Case 4.

Figure 12. - Design spanwise variations in shell permeability-tc-thickness ratio for wire-shell blade.